Cell Repolarization Variability Modulates Atrial Fibrillation Dynamics in 3D Virtual Human Atria

C Sánchez[1,2,3], A Bueno-Orovio[4], E Pueyo[2,1], B Rodríguez[3]

[1] Aragón Institute of Engineering Research, IIS Aragón, University of Zaragoza, Zaragoza, Spain
[2] CIBER de Bioingeniería, Biomateriales y Nanomedicina (CIBER-BBN), Zaragoza, Spain
[3] Department of Computer Science, University of Oxford, Oxford, UK
[4] Oxford Centre for Collaborative and Applied Mathematics, University of Oxford, Oxford, UK

Abstract

Intersubject variability in cardiac electrophysiology might determine the patient-specific proneness to suffer and/or sustain arrhythmia episodes, such as atrial fibrillation (AF). However, its potential influence on arrhythmogenesis is not well understood. In this study, we compare AF activity in virtual 3D human atria models with notable differences in cellular repolarization dynamics, in order to investigate mechanisms of intersubject variability. Physiological populations of models representing myocytes of patients with chronic AF were obtained and divided into sub-populations depending on the action potential duration (APD) measured at 90%, 50% and 20% repolarization. Each sub-population was used to build a model of the human atria. Analysis of calculated pseudo-electrograms showed the dominant frequency was in general higher for the short APD than for the long APD sub-populations. Organisation indices presented similar values for both APD_{90} sub-populations, whereas they were higher for the short APD_{50} and APD_{20} sub-populations, respectively. Regularity indices were lower for the short APD sub-populations. In conclusion, our results indicate that patients with long atrial APD could be associated with slow but very regular fibrillatory patterns, whereas short APDs may entail high frequency reentrant rotors and larger organisation.

1. Introduction

Reentrant circuits are one of the main mechanisms sustaining the most commonly diagnosed arrhythmia: atrial fibrillation (AF). AF presents chaotic activation patterns with some reentrant circuits coexisting around different rotors. Chronic AF (cAF) is associated with electrical remodeling of cardiac tissue involving short refractory periods and slow conduction, which favor reentry.

There is great variability in cardiac electrophysiology between patients, which may underlie the different biological proneness to suffer AF episodes. This electrophysiological variability entails differences in the electrical signals that can be measured on the atrial wall, such as the electrograms (EGM). The understanding and characterization of EGM attributes are key to properly apply the most appropriate anti-AF therapy for each patient.

The aim of this study is to analyze arrhythmogenic substrates in realistic anatomical human atrial models [1], under scenarios of cAF, and investigate the implications of notable differences in their cellular repolarization dynamics. A population of cellular models based on the Maleckar *et al.* action potential (AP) model [2], calibrated to fit experimental observations in cAF patients, was built to represent and include intercellular variability in atrial electrophysiology in the 3D models of human atria. Out of the whole population, sub-populations were extracted according to their AP duration (APD at 90, 50 and 20% repolarization), so that the effects of differences in the dynamics of each repolarization stage on arrhythmia-related markers could be assessed.

2. Methods

2.1. Cell model population

The human atrial AP model developed by Maleckar *et al.* [2] was used for description of atrial cell electrophysiology. Electrical remodeling associated with cAF was simulated by altering ion channel conductances as described in previous studies [3]: 50% I_{CaL} reduction; 70% I_{to} reduction; 50% I_{Kur} reduction; and 100% I_{K1} increment. A population of human atrial cell models models was generated by simultaneously modifying ionic current conductances within $\pm$30% range from median physiological values, obtaining 2275 combinations, and was then calibrated to fit experimental observations in cAF patients [4,5]. Out of the obtained population (Figure 1A), sub-populations were extracted according to their APD measured at 90%, 50% and 20% repolarization, separating those models over the third quartile from those below the first quartile (Figure 1, panels B-D).

Table 1. Tissue anisotropy and heterogeneities.

	Anisotropic ratio	CV (cm/s)	I_{to}*	I_{CaL}*	I_{Kr}*	I_{KACh}*
LA	1:2	59	1	1	$\sqrt{1.6}$	$\sqrt{2}$
RA	1:2	59	1	1	$1/\sqrt{1.6}$	$1/\sqrt{2}$
SAN	1:1	31	1	1	1	1
CT	1:10	116	1.35	1.6	0.9	1
PM	1:2	98	1.05	0.95	0.9	1
FO, RAPG, IAB	1:2	59	1	1	1	1
BB	1:2	98	1	1	1	1
CTI	1:1	44	1	1	1	1
LAPG	1:2	59	0.65	1.05	2.75	1
AVR	1:2	59	1.05	0.65	3	1

*Multiplicative factors with respect to default values in each model of the sub-populations

Effects of parasympathetic stimulation were simulated by including 1 nM of acetylcholine concentration ([ACh]) in all the simulations through an ACh-activated potassium current (I_{KACh}) [2].

2.2. 3D atrial model

The 3D model, which was developed at the Karlsruhe Institute of Technology, contains the main atrial structures: left atrium (LA), right atrium (RA), sinoatrial node (SAN), cresta terminalis (CT), pectinate muscles (PM), fossa ovalis (FO), Bachmann's bundle (BB), cavotricuspid isthmus (CTI), left atrial appendage (LAPG), right atrial appendage (RAPG), atrioventricular ring (AVR) and interatrial bridges (IAB). Furthermore, the model includes fiber orientation, conduction anisotropy and spatial heterogeneities in both ionic currents and conduction velocity (CV) [1]. Anisotropic ratio (transversal to longitudinal ratio of conductivity) and spatial heterogeneities are summarized in Table 1. LA-RA gradients were simulated by including differences in I_{Kr} (1.6 times larger in LA than RA) and I_{KACh} (2 times larger in LA than RA) according to previous studies [6].

One 3D cAF default model without repolarization variability and six 3D sub-population models with repolarization variability were used. For each of those six models, each cell in the virtual 3D model was randomly assigned a model of the corresponding sub-population described in 2.1, maintaining the electrophysiological heterogeneities shown in Table 1.

2.3. Stimulation protocol

A preliminary conditioning of the 3D model was performed by applying a train of 40 periodic stimuli at the SAN cells at a cycle length of 500 ms. Then, 6 extra-stimuli were applied around the right pulmonary veins (RPV) to generate reentries and fibrillatory behavior. Stimuli were 2-ms duration and twice diastolic threshold current pulses. Simulations were run with the software Elvira,

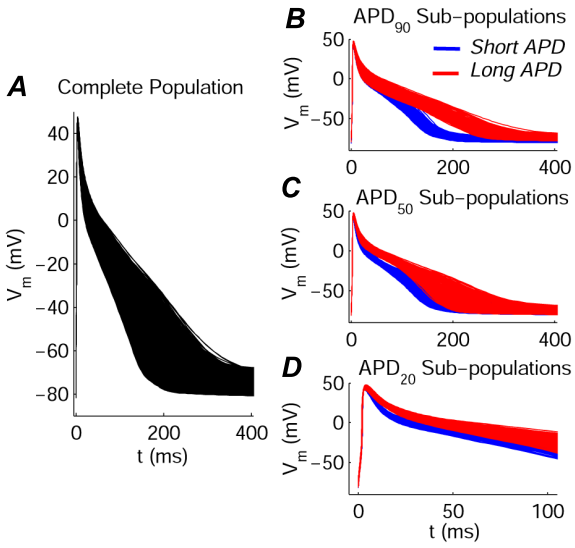

Figure 1. **A:** Population of simulated cAF cell models. **B**, **C** and **D:** First (blue) and fourth (red) quartile sub-populations according to APD_{90}, APD_{50} and APD_{20}, respectively.

which uses the finite element method described in [7].

2.4. Arrhythmic markers in AF

LA and RA were mapped with 49 virtual electrodes, separated approximately 1 cm from their closest neighbor and 0.1 cm from the atrial surface. Pseudo-electrograms (pEGMs) were calculated at each of these electrodes [8]. The following properties were measured on the pEGMs to characterize arrhythmic activity: (i) dominant frequency (DF); (ii) spectral organisation index (OI), which reflects the complexity of AF by relating the area under the DF and its harmonics to the total spectral power [9]; and (iii) regularity index (RI), which measures morphological sim-

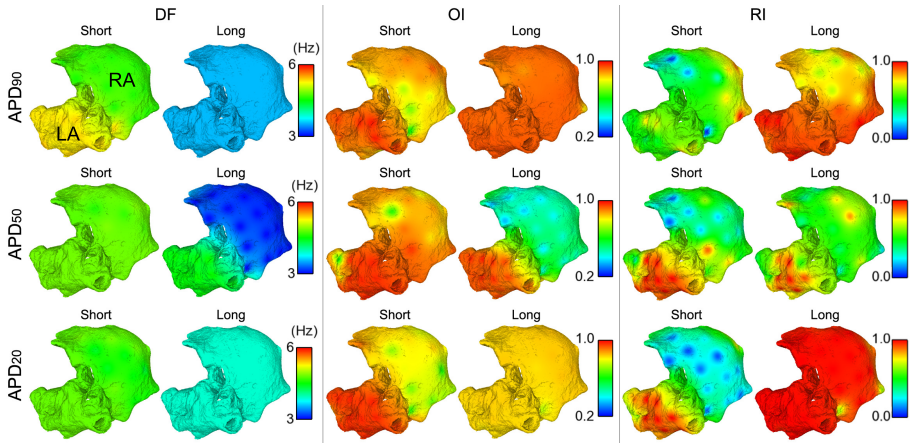

Figure 2. Dorsal view of the atria. Interpolated maps of dominant frequency (DF), organisation index (OI) and regularity index (RI) for long and short APD_{90}, APD_{50} and APD_{20} sub-populations of models, respectively.

ilarity of the electrical activations in a pEGM [10].

Regarding the analysis of calcium dynamics, the time course of the intracellular calcium concentration was obtained at the 49 closest atrial surface points to the virtual electrodes. Then, both the average of the calcium transient duration (CaT) and the average of the maximum diastolic calcium concentration (CaT_{max}) were calculated.

3. Results

3.1. Reentrant properties

Simulated arrhythmia with the default cAF model without repolarization variability was sustained by two main reentrant rotors located near RPV and RAPG. DF distribution throughout the tissue was almost uniform due to the highly stable rotors in each atrium, but DF was on average 0.69 Hz higher in LA than in RA (5.52 vs. 4.81 Hz). Regarding OI and RI, both markers exhibited higher values in LA: OI was above 0.8 in both atria, whereas RI was more heterogenous taking high values near RPV (0.75), but lower than 0.3 in areas around BB and RAPG. These areas with low RI are associated to either propagation block or collision between wavefronts. Regarding calcium dynamics, CaT was about 156 ms in LA and 181 ms in RA, while CaT_{max} was about 40 μM in all the tissue except for RAPG where it was sightly above 50 μM.

3.2. Repolarization variability effects

Comparing short vs. long APD_{90}, propagation was chaotic with some reentrant rotors coexisting for the short APD_{90} subpopulation, whereas fibrillatory activity was sustained by one rotor in RA for the long APD_{90} sub-population. DF was higher for the short APD_{90} sub-population, particularly in LA, OI was high for both sub-populations and RI was very low in most of the tissue for the short APD_{90} sub-population, but notably high for the

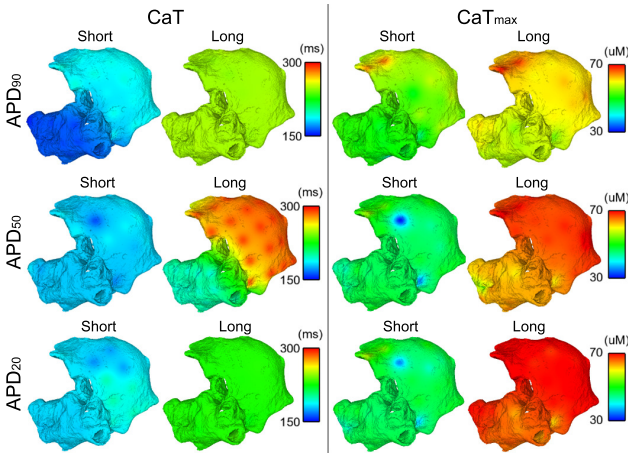

Figure 3. Dorsal view of the atria. Interpolated maps of CaT and CaT_{max} for long and short APD_{90}, APD_{50} and APD_{20} sub-populations of models, respectively.

long APD_{90} sub-population (Figure 2). Regarding calcium dynamics, the short APD_{90} sub-population showed much shorter CaT, but only slightly lower CaT_{max} with respect to the long APD_{90} sub-population (Figure 3).

Short and long APD_{50} simulations showed significant differences in both DF and OI calculated in RA, due to inter-atrial propagation block occurring in one out of three wavefronts from LA to RA for the long APD_{50} simulation. However, RI was similar between both scenarios (Figure 2). Calcium transients also showed notable differences between both simulations, being much longer and reaching higher concentrations for the long APD_{50} case (Figure 3).

Finally, simulations with short and long APD_{20} sub-populations showed notable dissimilarities in the fibrillatory pattern. The simulation with short APD_{20} behaved similarly to that with short APD_{50}, but with a more chaotic

propagation in RA, as shown by the lower values of both OI and RI (Figure 2). Regarding the long APD_{20}, there was only one main rotor, with low DF, high OI and high RI in all the tissue (Figure 2), which stopped propagating after 6.3 seconds of simulation due to inter-atrial conduction block. Calcium transient was homogeneously distributed in both simulations, but significantly shorter and reaching lower maximum concentration for short APD_{20} (Figure 3).

4. Discussion and conclusions

In this study seven whole human atrial models with specific variability in cell repolarization dynamics were used to assess the relevance of electrophysiological variability in AF characteristics. A more heterogenous tissue can be associated with slower reentrant circuits, thus favoring the generation of secondary rotors and wavelets [11]. Simulations show notable differences in fibrillatory behavior between rapid and slow repolarization dynamics, highly dependent on the stages of atrial cell repolarization.

Differences in the final phase of repolarization (APD_{90}) lead to significant changes in the fibrillatory pattern and therefore in the modulation of DF, RI and CaT, in good agreement with the effects of pharmacological interventions targeting ionic currents involved in this phase, such as I_{K1}, I_{NaK}, I_{Kr} or I_{Ks} [12].

Differences in the middle repolarization phase (APD_{50}) highly influence the propagation pattern, including inter-atrial conduction block when APD_{50} is long, thus leading to significant inter-atrial differences in DF, OI, and CaT. CaT_{max} is strongly modulated by APD_{50} variability, as expected by the role of I_{CaL} in this repolarization phase.

Analysis of the initial phase of repolarization (APD_{20}) is similar to that in the middle phase, with the exception of the total propagation block of the reentrant circuit when the APD_{20} is long. Differences in RI and CaT_{max} are explained by to the role of ionic currents involved in this repolarization phase, particularly I_{to}, I_{Kur} and I_{CaL}.

This study contributes to improve our understanding of concurrent mechanisms promoting and maintaining AF, focusing on cellular repolarization. Our simulations show patients with long atrial APD could be associated with slow but very regular fibrillatory patterns, whereas short APDs may entail high frequency reentrant rotors and larger organisation.

Acknowledgements

This study was financially supported by grant TEC-2010-19140, from Ministerio de Economía y Competitividad (MINECO), Spain, and CIBER de Bioingeniería, Biomateriales y Nanomedicina through Instituto de Salud Carlos III and FEDER, Spain (to C.S. and E.P.). E.P. acknowledges the financial support of Ramón y Cajal program from MINECO. A.B.O. is supported by Award No. KUK-C1-013-04, made by King Abdullah University of Science and Technology (KAUST). B.R. holds MRC Career Development, Industrial Partnership and Centenary Awards. The study was technically possible thanks to Gunnar Seemann, Martin Krueger, Olaf Dössel, from Karlsruhe Institute of Technology; Ursula Ravens, Erich Wettwer, from Dresden University of Technology; and José Félix Rodríguez, from University of Zaragoza.

References

[1] Seemann G *et al.*: Heterogeneous three-dimensional anatomical and electrophysiological model of human atria. Phil Trans R Soc A 2006;364:1465–1481.

[2] Maleckar MM *et al.*: K^+ current changes account for the rate dependence of the action potential in the human atrial myocyte. Am J Physiol Heart Circ Physiol 2009;297:H1398–H1410.

[3] Grandi E *et al.*: Human atrial action potential and Ca^{2+} model: sinus rhythm and chronic atrial fibrillation. Circ Res 2011;109:1055–1066.

[4] Wettwer E *et al.*: The new antiarrhythmic drug vernakalant: ex vivo study of human atrial tissue from sinus rhythm and chronic atrial fibrillation. Cardiovasc Res 2013;98:145–154.

[5] Britton OJ *et al.*: Experimentally calibrated population of models predicts and explains intersubject variability in cardiac cellular electrophysiology. Proc Natl Acad Sci USA 2013;110:E2098–E2105.

[6] Atienza F *et al.*: Activation of inward rectifier potassium channels accelerates atrial fibrillation in humans: evidence for a reentrant mechanism. Circulation 2006;114:2434–2442.

[7] Heidenreich EA *et al.*: Adaptive macro finite elements for the numerical solution of monodomain equations in cardiac electrophysiology. Ann Bio Eng 2010;38:2331–2345.

[8] Baher A *et al.*: Short-term cardiac memory and mother rotor fibrillation. Am J Physiol Heart Circ Physiol 2007;292:H180–H189.

[9] Everett TH *et al.*: Frequency domain algorithm for quantifying atrial fibrillation organization to increase defibrillation efficacy. IEEE Trans Biomed Eng 2001;48:969–978.

[10] Faes L and Ravelli F: A morphology based approach to the evaluation of atrial fibrillation organization. IEEE Eng Med Biol Mag 2007;26:54–59.

[11] Wijffels MCEF *et al.*: Widening of the excitable gap during pharmacological cardioversion of atrial fibrillation in the goat: effects of cibenzoline, hydroquinidine, flecainide, and d-sotalol. Circulation. 2000;102:260–267.

[12] Sánchez C *et al.*: The Na^+/K^+ pump is an important modulator of refractoriness and dynamics in human atrial tissue. Am J Physiol Heart Circ Physiol 2012;302:H1146–H1159.

Address for correspondence:

Carlos Sánchez
DIEC / I3A / University of Zaragoza / Spain
cstapia@unizar.es